Laboratory Identification of Probable Interstellar Dust Particles Collected by the Stardust Spacecraft

Andrew J. Westphal,[1*] Rhonda M. Stroud,[2] Hans A. Bechtel,[3] Frank E. Brenker,[4] Anna L. Butterworth,[1] George J. Flynn,[5] David R. Frank,[6] Zack Gainsforth,[1] Jon K. Hillier,[7] Frank Postberg,[7] Alexandre S. Simionovici,[8] Veerle J. Sterken,[9] Larry R. Nittler,[10] Carlton Allen,[11] David Anderson,[1] Asna Ansari,[12] Saša Bajt,[13] Ron K. Bastien,[6] Nabil Bassim,[2] John Bridges,[14] Donald E. Brownlee,[15] Mark Burchell,[16] Manfred Burghammer,[17] Hitesh Changela,[18] Peter Cloetens,[19] Andrew M. Davis,[20] Ryan Doll,[21] Christine Floss,[21] Eberhard Grün,[22] Philipp R. Heck,[12] Peter Hoppe,[23] Bruce Hudson,[24] Joachim Huth,[23] Anton Kearsley,[25] Ashley J. King,[20] Barry Lai,[26] Jan Leitner,[23] Laurence Lemelle,[27] Ariel Leonard,[21] Hugues Leroux,[28] Robert Lettieri,[1] William Marchant,[1] Ryan Ogliore,[29] Wei Jia Ong,[21] Mark C. Price,[16] Scott A. Sandford,[30] Juan-Angel Sans Tresseras,[19] Sylvia Schmitz,[4] Tom Schoonjans,[17] Kate Schreiber,[21] Geert Silversmit,[17] Vicente A. Solé,[19] Ralf Srama,[31] Frank Stadermann,[21] Thomas Stephan,[20] Julien Stodolna,[1] Stephen Sutton,[26] Mario Trieloff,[7] Peter Tsou,[32] Tolek Tyliszczak,[3] Bart Vekemans,[17] Laszlo Vincze,[17] Joshua Von Korff,[1] Naomi Wordsworth,[33] Daniel Zevin,[1] Michael E. Zolensky,[11] 30714 Stardust@home dusters[34]

[1] Space Sciences Laboratory, U. C. Berkeley, Berkeley, CA USA, [2] Materials Science and Technology Di- vision, Naval Research Laboratory, Washington, DC USA, [3] Advanced Light Source, Lawrence Berkeley Laboratory, Berkeley, CA USA, [4] Geoscience Institute, Goethe University Frankfurt, Frankfurt, Germany, [5] SUNY Plattsburgh, Plattsburgh, NY USA, [6] ESCG, NASA JSC, Houston, TX USA, [7] Institut für Geowis- senschaften, University of Heidelberg, Germany, [8] Institut des Sciences de la Terre, Observatoire des Sciences de l'Univers de Grenoble, Grenoble, France, [9] IRS, University of Stuttgart, Stuttgart, Germany; IGEP, TU Braunschweig, Braunschweig, Germany; Max Planck Institut für Kernphysik, Heidelberg, Germany and International Space Sciences Institute, Bern, Switzerland, [10] Carnegie Institution of Washington, Washington, DC USA, [11] ARES, NASA JSC, Houston, TX USA, [12] Field Museum of Natural History, Chicago, IL USA, [13] DESY, Hamburg, Germany, [14] Space Research Centre, University of Leicester, Leicester, UK, [15] Department of Astronomy, University of Washington, Seattle, WA USA, [16] University of Kent, Canterbury, Kent, UK, [17] University of Ghent, Ghent, Belgium, [18] University of New Mexico, [19] European Synchrotron Radiation Facility, Grenoble, France, [20] University of Chicago, Chicago, IL USA, [21] Washington University, St. Louis, MO USA, [22] Max-Planck-Institut für Kernphysik, Heidelberg, Germany, [23] Max-Planck-Institut für Chemie, Mainz, Germany, [24] 615 William St., Apt 405, Midland, Ontario, Canada, [25] Natural History Museum, London, UK, [26] Advanced Photon Source, Argonne National Laboratory, Lemont, IL USA, [27] Ecole Normale Superieure de Lyon, Lyon, France, [28] University Lille 1, France, [29] University of Hawai'i at Manoa, Honolulu, HI USA, [30] NASA Ames Research Center, Moffett Field, CA USA, [31] IRS, University Stuttgart, Stuttgart, Germany, [32] Jet Propulsion Laboratory, Pasadena, CA USA, [33] Wexbury, Farthing Green Lane, Stoke Poges, South Buckinghamshire, UK, [34] Worldwide

*Corresponding author

Deceased

Abstract

Seven particles captured by the Stardust Interstellar Dust Collector and returned to Earth for laboratory analysis have features consistent with an origin in the contemporary

interstellar dust stream. More than 50 spacecraft debris particles were also identified. The interstellar dust candidates are readily distinguished from debris impacts on the basis of elemental composition and/or impact trajectory. The seven candidate interstellar particles are diverse in elemental composition, crystal structure and size. The presence of a significant crystalline component and multiple iron-bearing phases, including sulfide, in some particles indicates that individual interstellar particles diverge from the average properties of interstellar dust inferred from astronomical observations and modeling.

Summary: Laboratory analyses of seven particles captured by the Stardust Interstellar Dust Collector reveal the diverse properties of individual interstellar dust particles.

Interstellar dust (ISD) from the local interstellar medium (LISM) streams into the solar system from approximately the direction of the constellation Ophiuchus. Prior to the return of the NASA Stardust spacecraft (*1*) no recognizable samples of this interstellar dust were available for laboratory study. Thus, our understanding of the properties of contemporary ISD has been derived primarily from astronomical observations of the ISM, including optical properties of the ISD and remote spectroscopy of the gas composition (*2-4*), and from *in situ* measurements by the dust analyzers on the Cassini, Ulysses and Galileo spacecraft (*5-7*). The canonical picture of ISD is that it is dominated by ~0.2 μm diameter (*8*) amorphous silicate grains, with or without carbonaceous mantles. However, the inferred properties of the particles, including size distribution, density and composition are heavily model dependent.

Direct, laboratory-based measurement of returned ISD offers an independent test of the assumptions on which the interpretation of spectroscopy and *in situ* dust measurements rest. Important questions to be addressed include: is there one dominant dust phase, and if so, what is its composition? Is the dominant structure crystalline or amorphous? Is iron present in metal, oxide, carbide and/or sulfide phases? Are the particles dense or fluffy? Is there evidence for particle mantles of either organic or silicate-like composition? We present here results from the Stardust Interstellar Preliminary Examination (ISPE), in which we have identified seven dust particle impacts of probable interstellar origin, in order to address these and related questions. The identification of these seven impacts is the result of a massively-distributed, volunteer-based, search of optical micrographs of the aerogel collectors, manual and automated searches of scanning electron micrographs of aluminum foils, extensive coordinated sample analyses, laboratory hypervelocity impact experiments, and numerical modeling of ISD propagation in the heliosphere. These are described in detail in a series of papers (*9-20*) published contemporaneously with this article; further supplementary details can be found on *Science* online *(21)*.

The 0.1 m^2 Stardust Interstellar Dust Collector (SIDC) consisted of an Al frame holding ultra-low density silica aerogel tiles (*1*) that constitute 85% of the exposed area, and Al foils that

constitute the remaining 15%. The collector was exposed to the interstellar dust stream for 195 days in two periods in 2000 and 2002. The low density of the silica aerogel enables capture of hypervelocity particles with mild deceleration as compared with other capture media, to limit the capture alteration effects, while simultaneously recording particle trajectory in the form of a carrot-shaped track. The optical transparency of the aerogel allows for detection of tracks ≥ 2 μm in diameter (*9*). The Al foil is a complementary collection medium to the silica aerogel. Impact residues on the foils are localized to craters on the surface, which contain residue that is not mixed with silica aerogel. Scanning electron microscopy of the foils can identify impact craters as small as 0.3 μm in diameter, corresponding to ~0.2 μm diameter particles.

The criteria for identifying candidate interstellar particles (Table S1) in the two collection media are slightly different. The first order criteria (levels 0-2) are that the shape of the identified feature must be consistent with hypervelocity impact, and the captured particle or particle residue must have a composition that is consistent with formation in space, and inconsistent with spacecraft materials, or aerogel impurities. The trajectory of the particle is taken into consideration for the samples collected in aerogel, but not for the foils, because crater shapes depend strongly on the particle shape and composition, in addition to trajectory (*22*). The most definitive indication of an interstellar origin (level 3) for a particular particle would be an oxygen isotope composition inconsistent with solar system values. However, the converse is not true—an oxygen isotope composition within the range of solar system values does not uniquely constrain the origin to the solar system. All seven of the captured particles reported here are level 2 candidates, for which the oxygen isotope data are either not yet available, or are consistent with solar values. This means that although an interstellar origin cannot be definitively proven for the particles, other origins, including as interplanetary dust, have been determined to be statistically less likely than an interstellar origin. Three interstellar candidates were identified in a search of ~250 cm^2 of the exposed aerogel and four interstellar candidates were identified in a search of ~5 cm^2 of the exposed Al foil.

Identification and analysis of candidates in aerogel

We identified 71 tracks in an examination of slightly over half of the aerogel tiles in the SIDC. All but two were identified through the Stardust@home project (*9, 10*), in which volunteers searched online for tracks in digital micrographs of the aerogel collector. We extracted a subset of these tracks in volumes of aerogel, called “picokeystones” (*10, 23*), and mounted them between 70 nm-thick Si_3N_4 membranes to protect from loss and contamination. Picokeystones were subsequently analyzed at one or more of six synchrotrons with techniques including Scanning Transmission X-ray Microscopy (STXM) (*12*), Fourier Transform Infrared Spectroscopy (FTIR) (*11*), X-Ray Fluorescence spectroscopy (XRF) (*13-15*) and X-Ray Diffraction (XRD) (*16*). Forty-six of the tracks are consistent in their trajectories with an origin as secondary ejecta from impacts on the aft solar panels and this origin was confirmed for four (*12-15*) by the presence of cerium, a cosmically rare element present in the glass covering the spacecraft solar panels. The remaining 25 so-called “midnight” tracks have trajectories that are

consistent with an origin either in the interstellar dust stream or as ejecta from impacts on the lid of the sample return capsule (*20*). The ambiguity in origin of these 25 is due to the articulation of the collector on its arm during the exposure (*24*). Because of the extremely limited amount of sample, we analyzed only the first 13 midnight tracks identified. Six showed aluminum X-ray Absorption Near-Edge spectra (XANES) consistent with Al metal. These tracks are consistent with Al ejected from the sample return capsule by micrometeoroid impacts. Three tracks showed heavy element abundances that pointed away from an extraterrestrial origin, and one was not analyzable because of unusually high aerogel density. We focus here on three midnight tracks that are consistent with an extraterrestrial origin.

I1043,1,30,0,0 ("Orion") (Fig. 1) is a multicomponent, low-density 3.2±0.1(systematic)±0.4 (instrumental) pg particle compositionally consistent with a mixture of forsteritic olivine (Mg_2SiO_4, 19±3 mol%), magnesium-spinel ($MgAl_2O_4$, 27±2 mol%), and iron-bearing phases (assumed to be Fe/FeO, 45±3 mol% and FeS, 2.2±0.4 mol%) plus 6.4±0.6 mol% in minor elements calcium, chromium, manganese, and nickel. Further composition details and discussion of errors are available *[21]*. XRD and STXM analyses show a good fit to polycrystalline olivine with mosaiced domains showing broadening in x-ray diffraction extending over 20º, nanocrystalline spinel, two undetermined crystalline phases of unknown composition, and an amorphous magnesium, aluminum oxide phase. One of the unidentified crystalline phases is consistent with iron metal nanoparticles. We derived an average density of ~0.7 g cm^{-3}. Elemental abundances normalized to magnesium and the composition of CI meteorites, whose abundances of nonvolatile elements are nearly identical to those of the Sun, and hence the bulk Solar System, show ten-fold enrichments in aluminum and the minor element copper, depletions for silicon, calcium and near normal iron, chromium, manganese, and nickel. Magnesium was used for normalization rather than the more usual silicon since its abundance could be measured precisely by STXM, whereas the silicon abundance is less certain due to the silica aerogel background. Comparison of the Orion track morphology with hypervelocity analog shots (*17*) indicates a capture speed <10 km s^{-1}.

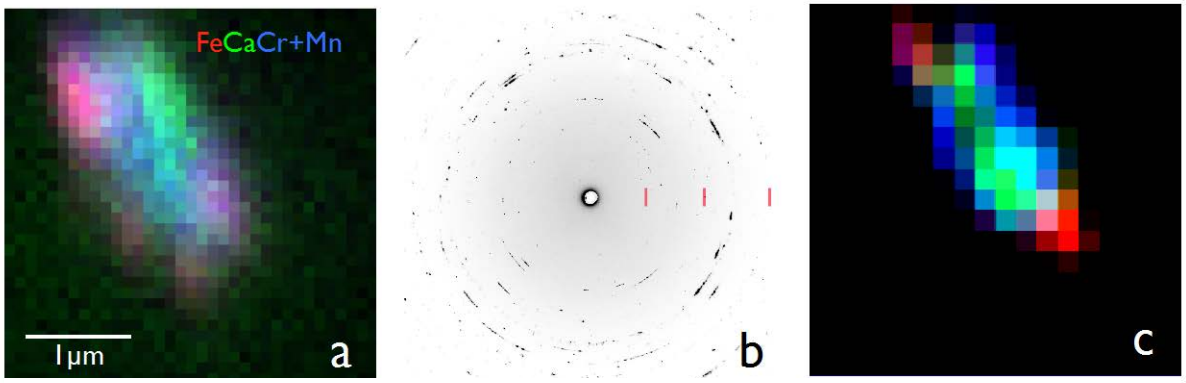

Fig. 1. (a) Tri-color iron, calcium, (chromium+manganese) elemental map of Orion derived from XRF data. Colors are scaled to span the entire range of each element. (b) XRD pattern of Orion taken at 13.9 keV. Tick marks at d-spacings of 6Å, 3Å, and 2Å are indicated. (c) Phase map of Orion. Green is olivine, red is spinel, and blue is an unidentified phase.

I1047,1,34,0,0: ("Hylabrook") (Fig. 2) is a magnesium-, iron-, and silicon-rich ~4 pg particle with a mosaiced, partially amorphized, 0.6 µm^3 forsteritic (Mg/(Mg+Fe) >80) olivine core (30 mol%) surrounded by a low density halo compositionally modeled by disordered magnesium-silicate (Mg_2SiO_4, 1 mol%), amorphous oxidized aluminum (Al_2O_3, 2 mol%), amorphous metal oxides (Cr_2O_3, 8 mol%, MnO, 5 mol%), and an iron-bearing phase (Fe/FeO, 54 mol%), which may include reduced iron nanoparticles. The overall density of the particle (as captured) was ~0.3 g cm^{-3}. The major elements magnesium, silicon and iron are present in CI-like relative proportions; magnesium-normalized elemental abundances show depletions in calcium and nickel, and enrichments in chromium, manganese, and copper, relative to CI. XRD data provide a good match to mosaiced olivine with an internal strain field up to 0.3%. The magnesium XANES spectrum shows that magnesium is present both in Hylabrook's crystalline core and in a partially amorphized olivine shell. The morphology of the track indicates that Hylabrook was also captured at <10 km s^{-1} (*17*).

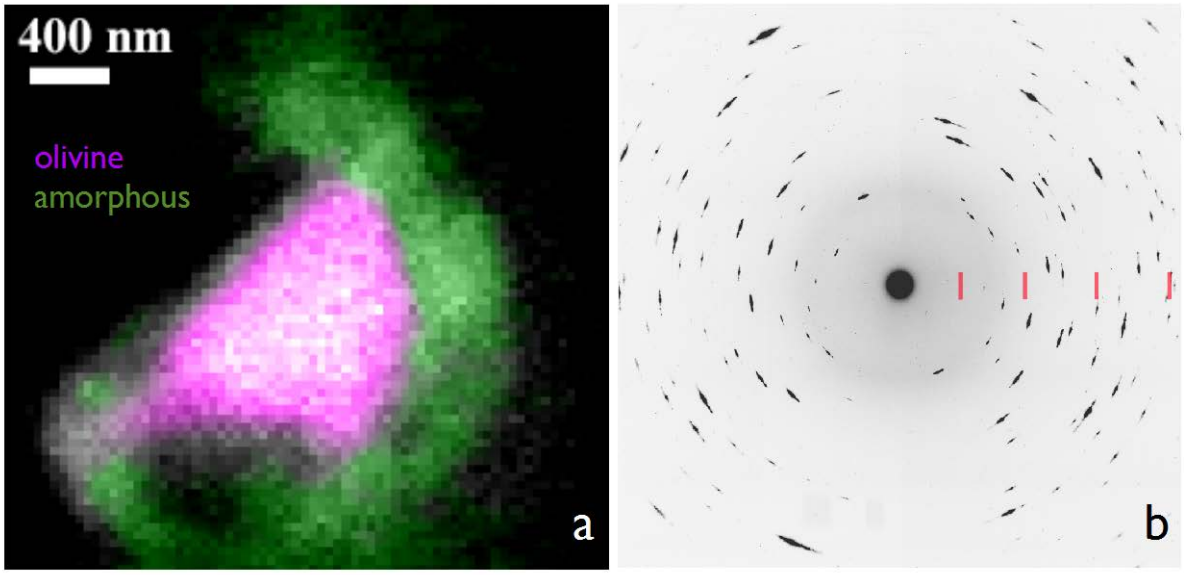

Fig. 2. (a) Bi-color olivine + amorphous phase map of Hylabrook derived from STXM Mg XANES data. (b) XRD pattern of Hylabrook taken at 13.9 keV. Tick marks at d-spacings of 6Å, 3Å, 2Å, and 1.55Å are indicated.

Comparison of the morphology of track I1003,1,40,0,0 ("Sorok") with laboratory experiments (*17*) indicates that the capture speed was >15 km s^{-1}, and that the original projectile had a mass of ~3 pg (Fig. 3). Silicon and carbon were detected in the track walls, but it is not clear whether the carbon is projectile residue, or carbon indigenous to the compressed aerogel, since carbon contamination is known to be present in the Stardust aerogel collectors (*25*). Organic materials are below detection limits in an FTIR analysis. Magnesium and aluminum were below detection limits in STXM analysis. If this particle had similar iron contents to Orion or Hylabrook and the entire particle residue were retained in the track, iron should have been detectable with STXM in the track walls. The nondetection of iron implies that either the original projectile was relatively iron-poor compared to Orion and Hylabrook, or that relatively little of the original projectile was retained in the track.

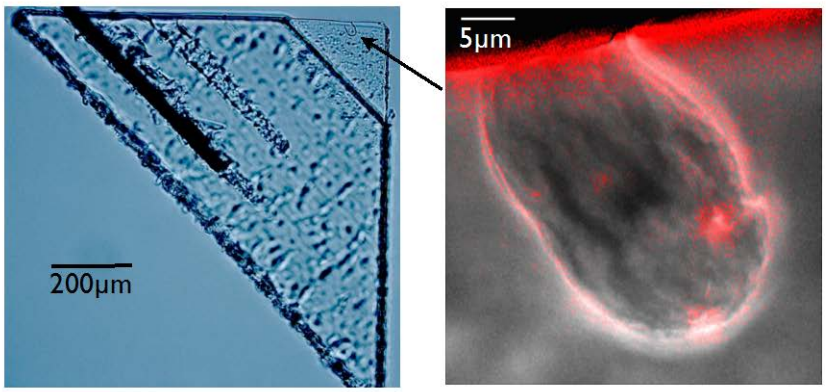

Fig. 3. (left) Optical micrograph of I1003,1,40,0,0 ("Sorok") in its picokeystone. (right) STXM absorption map at 280 eV with overlaid map of carbon (red).

Identification and analysis of candidates on the aluminum foil

We identified 25 crater-like features after an automated scanning electron microscope-based search of 13 individual Al foils (*19*). Elemental analysis, by either Auger electron spectroscopy or energy dispersive X-ray spectroscopy (EDS), indicates that most of these features are impacts from fragments of the spacecraft solar panels. These craters contain residues rich in elements that are associated with the solar panel cover glass (boron, cerium, zinc, and titanium) and antireflection coating (fluorine), and that are of low cosmic abundance. Five of the features are associated with native defects in the foil, and are not impact craters. Four of the impact craters contain residues with compositions inconsistent with spacecraft origin or native foil defects. The diameter of these candidate interstellar craters ranges from 0.28 μm to 0.46 μm. The crater diameter (D_c) is a function of particle diameter (D_p), capture speed and density (*26, 27*), with $D_c \sim 1.6D_p$ for silica spheres impacting Al_{1100} alloy at 6.1 km s^{-1}. Thus, the diameters of the particles that produced the craters range from ~0.2 to 0.3 μm. We extracted cross-sections of these craters with focused ion beam milling, and then analyzed the cross-sections with scanning transmission electron microscopy (STEM) (*19*).

Dark-field STEM images and EDS maps of the cross-sections are shown in Fig. 4. The shape of the crater provides an indication of whether the impacting particle was a compact object with a single center of mass, or an aggregate with a few distinct centers of mass. The cross-sections of I1044N,3, I1061N,3, and I1061N,5 are consistent with one dominant center of mass. The residue in I1044N,3 consists of magnesium- and iron-rich silicate, with no detectable sulfur. The residue in I1061N,3 is dominated by iron-bearing, magnesium-rich silicate, and also contains FeS. The residue in crater I1061N,5 shows iron-bearing, magnesium-rich silicate on the left side of the crater, with iron metal and sulfide distributed across the crater and ~ 5 iron, nickel sulfide particles < 10 nm in diameter. The cross-section of I1061N,4 shows a double bowl shape, indicative of an aggregate impactor with two distinct mass centers. This is consistent with the composition of the retained residue that shows silicate on the left side of the crater, and iron, nickel metal and sulfide on the right side.

Oxygen isotopic ratios were measured by secondary ion mass spectrometry on two of the crater cross-sections *(21)* and found to be consistent with solar system values within errors (Table 1). Oxygen isotope measurements of the two other craters were not possible due to damage of the sections during transport between laboratories.

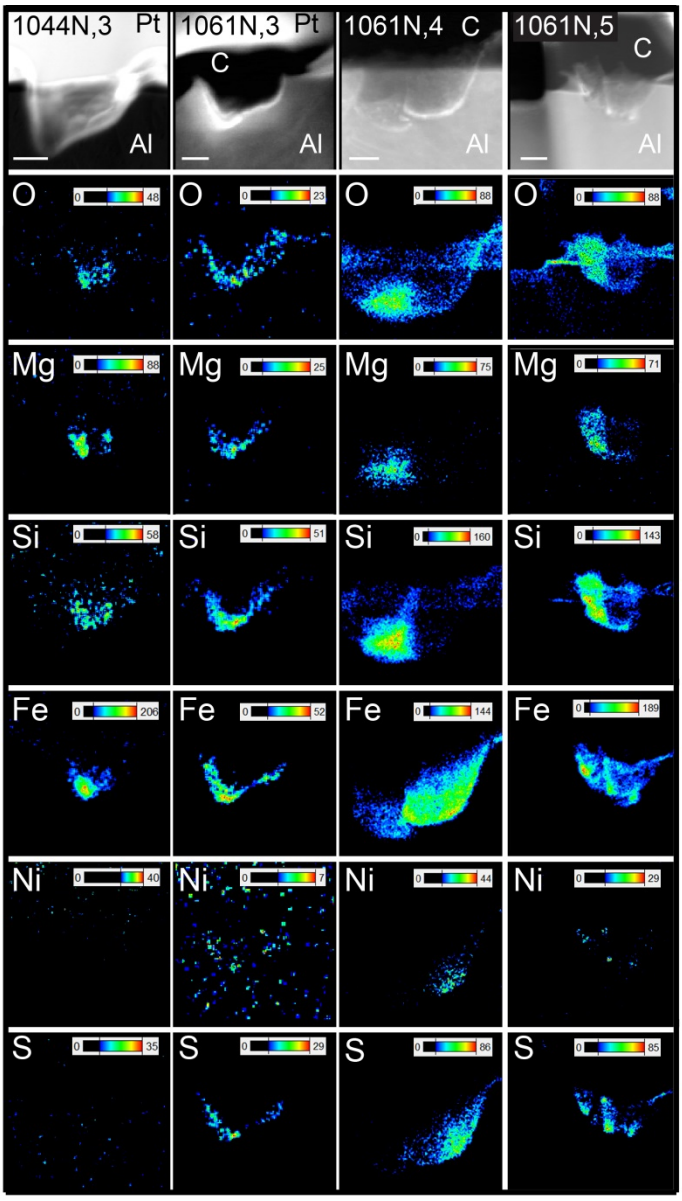

Fig. 4. Dark field STEM images and EDS-based element maps of the candidate interstellar craters. Scale bars indicate 100 nm.

Table 1. Summary of Interstellar Candidates

ID	Mass or Diameter	Composition	Structure	Capture Speed
I1043,1,30,0,0 ("Orion")	3.1 ± 0.4 pg	Forsteritic olivine core (Mg_2SiO_4, 19 mol%), + nanocrystalline spinel + amorphous ($MgAl_2O_4$, 27 mol%) + Fe-bearing phase (47 mol%) with 7 mol% minor elements Cr, Mn, Ni and Ca.	Low density, 0.7 g cm^{-3}	<10 km s^{-1}
I1047,1,34,0,0: ("Hylabrook")	4.0 ± 0.7 pg	Forsteritic ($Fo_{>80}$) olivine core (Mg_2SiO_4 30 mol%) surrounded by a low density halo including amorphous Mg-silicate (1 mol%) and Al-, Cr-, Mn- (15 mol%) and Fe-bearing (54 mol%) phases.	Low density (<0.4 g cm^{-3})	<10 km s^{-1}
I1003,1,40,0,0 ("Sorok")	~3 pg	Possible Si and C		> 15 km s^{-1}
I1044N,3	0.28 μm crater	Mg, Fe-rich silicate (Mg+Fe)/Si =3.3	Single particle with chemical zoning	>10 km s^{-1}
I1061N,3	0.37 μm crater	Silicate (Mg:Fe:Si = 0.58:0.22:1 at%) +FeS $\delta^{17}O = -13 \pm 30$ ‰, $\delta^{18}O = 11 \pm 13$‰, $^{18}O/^{17}O = 5.36 \pm 0.18$ (1σ errors)	Single particle or nanoscale aggregate	~ 5 to 10 km s^{-1}
I1061N,4	0.39 μm crater	Silicate (Mg:Fe:Si=0.33:0.15:1 at%) +Fe, Ni metal and sulfide	2 particle aggregate with zoning of metal and sulfide	~ 5 to 10 km s^{-1}
I1061N,5	0.46 μm crater	Silicate (Mg:Fe:Si 0.57:0.15:1 at%) +Fe metal and Fe, Ni sulfide $\delta^{17}O = -85 \pm 61$ ‰, $\delta^{18}O = -20 \pm 27$‰, $^{18}O/^{17}O = 5.61 \pm 0.36$ (1σ errors)	Nanoparticle aggregate	~ 5 to 10 km s^{-1}

Low probability of an interplanetary origin

The combination of the elemental compositions of the seven ISD candidates with their impact feature characteristics, i.e., track shape and direction, or crater morphology, demonstrates that they are extraterrestrial in origin. However, further information is needed to distinguish between a possible interplanetary origin and an interstellar origin. The determination of origin cannot be based on elemental composition alone, because of the similarity of the solar nebula and the LISM in gas composition, and the overlap in range of temperature and pressure conditions at which dust condenses. The products of gas-solid condensation in each environment will share some common phases, including amorphous and crystalline silicates, oxides, and potentially also sulfides. For example, a ubiquitous component of primitive, probably cometary, interplanetary dust particles (IDPs) consists of GEMS (glass with embedded metal and sulfides) particles, which are similar to the canonical ISD particle in size, composition, and lack of crystallinity in the silicate phase and thus have been argued to be preserved interstellar particles (*28*). However, the origin of GEMS remains highly controversial (*29*). Only a small fraction of GEMS particles have oxygen isotopic anomalies proving a circumstellar heritage, but particles formed in the ISM at the time of solar birth could have had solar isotopic signatures.

Three of the four crater ISD candidates show elemental compositions within the range reported for GEMS and two of these have solar-system-like oxygen isotopic ratios. The lack of strong oxygen isotopic anomalies rules out an origin in stellar outflows as inferred for meteoritic presolar grains. However, as with GEMS, normal oxygen isotopic composition does not preclude an origin in the ISM, since the range of isotopic compositions measured in the present-day ISM overlaps solar (Fig. S5). The fourth, I1044N,3, has a lower silicon and higher oxygen content than GEMS, and is thus more consistent with average values for the ISM dust composition (*3*). Orion and Hylabrook are distinct from GEMS in size, composition and/or degree of crystallinity, but both are composed of phases previously observed in interplanetary and circumstellar particles: Orion contains olivine and spinel-like amorphous oxide; the magnesium-rich amorphous content of Hylabrook appears to be a rim on an interior olivine, rather than a distinct amorphous silicate.

Because of the ambiguity in distinguishing interstellar and interplanetary origins on the basis of chemical and isotopic compositions, stronger constraints on the particle origin(s) come from the geometry of the Stardust interstellar collection. Modeling indicates that very few IDP impacts on the SIDC are expected to coincide with the “midnight” direction where interstellar impacts occur (*10,19)* and we observed no tracks in the angular range where IDPs should have their maximum flux, indicating that the IDP background is small. Based on the observed angular distribution of captured particles, and model trajectories, the statistical likelihood of an interplanetary origin for all three interstellar dust candidates in aerogel is <0.03% (*10,20)* The ecliptic longitude of the interstellar dust radiant that best fits the observed trajectories of the three candidates in aerogel is

somewhat larger than anticipated (*9, 18, 20*) based on observations from Ulysses and Galileo, but this may indicate a real long-term radiant shift which is consistent with the long-term increase in radiant longitude in neutral helium (*30*).

Although the trajectories of the four foil interstellar candidates are unknown, statistical arguments based on trajectories still apply. We used the Interplanetary Micrometeoroid Environment Model (IMEM) *(21,31)* to estimate the fluence of IDPs > 10^{-14}g collected to be 0.17 cm^{-2}. The observed impact density of the foils is 0.8 cm^{-2}, and thus the fraction of impacts of interplanetary origin is estimated to be 0.17/0.8= 0.2. This value is in good agreement with the preflight estimates of Landgraf et al. (32), who predicted a total collected particle count of 120 (80 < 2μm and 40 > 2μm diameter) interstellar particles and 20 IDPs. With the conservative assumption that all of the interplanetary dust is < 2 μm, this equates to 100 small particles (80 interstellar and 20 interplanetary), of which 20% should be interplanetary. Based on the good agreement of these two model calculations, we take 20% to be the probability of an interplanetary origin for any one impact, and < 0.16% to be the probability that all four craters are interplanetary in origin. The latter estimate assumes an uncorrelated origin for the impacting particles. A correlated origin as secondary ejecta from micrometeroid impacts on the sample capsule or solar cell array can be discounted because in the ejecta of such impacts, spacecraft material is expected to dominate over impactor material by approximately two orders of magnitude (*9,20*), and to have lower impact velocity and shallower impact depth than observed for interstellar candidate craters (*33*). This is inconsistent with the observed low ratio of target/projectile material in the impacts, even accounting for the low statistics (*34*), and the observed interstellar candidate crater morphologies. A correlated origin as fragments of asteroidal or other collisional products, can also be discounted. Such an origin would require a mechanism for maintaining correlated particle trajectories over large distances, against the differential solar light pressure and Lorentz forces that act on this size of particles. We conclude that an interstellar origin is most likely for the four candidate impact craters.

Implications for dust observations and modeling

Assuming that the captured particles are indeed all of interstellar origin, we can use their characteristics to address questions about the properties of contemporary interstellar dust. The particles in the aerogel and those in the foil sample two different size regimes. The particles captured in aerogel are > 1 μm diameter (~ 3 pg), which is consistent with the mass-wise dominant component of the dust sampled by *in situ* instruments on Ulysses and Galileo, but several hundred times more massive than the maximum dust size determined from observations of the ISM. The spectroscopic observations indicate a typical particle size of ~200 nm (~100 attograms for density ~2 g cm^{-3}). The particles captured in the Al foil are closer in size to that inferred for typical ISM particles by astronomical means. However, the *in situ* spacecraft data and models of heliospheric filtering (*18*) indicate that abundance of these particles is strongly

reduced at 2 A.U. compared to interstellar space than are the pg-sized grains (*35*). Compared to the predictions prior to the Stardust sample return, we observed an order of magnitude fewer large particles (pg-sized) and a factor of ~4 more small particles (attogram-sized) than expected from the *in situ* data.

The elemental compositions of the captured particles are generally consistent with expectations for ISD. Magnesium-rich silicates are common to all of the particles except Sorok, for which the actual particle composition could not be determined. In five of the particles (Orion, Hylabrook, and craters 1061N,3, 1061N,4 1061N,5), one or more distinct iron-rich phases were also observed. Some of the iron in Orion and Hylabrook may be in reduced form and three of the particles captured in foil show FeS, and possibly metallic Fe. The chemical form of iron in ISD is uncertain. Estimates of the iron content of interstellar silicates vary widely (e.g. (*36*)) and the variation in Fe:Mg gas depletions in different regions of the ISM indicate that one or more iron-rich dust phases distinct from the magnesium-rich silicate are expected. The particular phase or phases are not known, because they do not provide distinct features in the ISM IR spectra. Nanophase metallic Fe or FeS would be possible candidates, as both have broad, featureless IR spectra and these phases are ubiquitous components of primitive solar nebular materials and thus may also form as circumstellar and/or interstellar particles. The presence of a sulfide dust component in the ISM is a matter of significant debate. Most measurements of the ISM gas indicate little or no depletion of sulfur, compared to the solar abundance, which supports a lack of condensed sulfur-rich dust. However, uncertainty in determining the ISM gas-phase sulfur abundance, and the difficulty of detecting nanophase sulfides with IR spectroscopy do not rule out the possibility that FeS nanoparticles are a component of ISM dust (*37*).

The crystallinity of the silicates in Orion and Hylabrook is unexpected. Spectroscopic measurements of interstellar silicates indicate that < 2.2% are crystalline (*38, 39*). Irradiation of the particles by gas accelerated by shockwaves in the diffuse intercloud medium are believed to effectively amorphize silicates in typical (~100nm) ISD particles (*40*), but crystalline materials are probably preserved in the interiors of larger (>1μm) particles. Crystalline silicates are observed in the outflows of oxygen-rich AGB stars (*41*) and observed as preserved presolar circumstellar particles in IDPs (*42*) and meteorites (*43*). Since the fraction of the mass contained in particles as large as Orion and Hylabrook (> 3 pg) is << 1% of the condensed component of the ISM, the observation of crystalline material in them does not violate astronomical upper limits on silicate crystallinity (*38, 39*). The mineralogical complexity of Orion may be consistent with assembly from small crystalline and amorphous components in a cold molecular cloud environment, while Hylabrook may be consistent with a single processed circumstellar condensate. This hypothesis may be testable by a future measurement of the isotopic composition of oxygen. The residues of the particles captured in the Al foil appear to be amorphous, but it is unclear whether this is an original feature or an effect of hypervelocity capture alteration. Three of the four craters contain sulfides, while Orion contains only minor

sulfur and Hylabrook has no significant sulfur. This may be a further indication that larger particles sample a fundamentally different reservoir than small particles.

Optical and mechanical properties inferred from dust dynamics and statistics

Our measured fluence of >1μm diameter particles is ~ 1/10 of the prelaunch estimate (*32*). Because we used control images to measure detection efficiency in the Stardust collector, we can be confident that the difference is not due to detection inefficiency of high-speed impacts. However, the dynamics of nm- and μm-size particles in the heliosphere are strongly affected by radiation pressure exerted by sunlight. To investigate whether repulsion of interstellar dust by sunlight might play a role in reducing the flux in the inner solar system, we compared our observations of the track diameter distribution for our interstellar candidates with predictions of a model of interstellar dust propagation based on the Ulysses and Galileo (U/G) observations. We used a standard model of the optical properties of interstellar dust as a function of particle size (*5*), and the high-speed laboratory calibrations of interstellar dust analogs carried out as part of the present effort (*17*). We observed a dramatically lower flux of high-speed IS dust than predicted by this model (Fig. 5), but a model developed as part of the ISPE (*18*) in which the optical cross section of the dust is larger and which takes into account Lorentz forces, is consistent with the observations. Further, the standard model predicted that nearly all impacts would be at high speed (>>10 km sec^{-1}), because the model of optical properties assumed relatively compact, high-density dust particles. However, two of the three candidate impacts > 1 μm were captured with speeds << 10 km sec^{-1}. These observations can be most easily understood if interstellar dust in this size range consists of low-density material with a wide distribution of β, the ratio of radiation pressure force to gravitational force. Canonical ISD structures (*3*) consistent with such low-density particles include spheres with silicate cores and organic mantles, carbonaceous spheres, or aggregates of these. Of the seven candidate ISD particles, one is plausibly dominated by carbon, one is primarily a single silicate with a mantle-core structure, whereas the others are complex aggregates of various μm to nm-size phases such oxides, metal and sulfides, in addition to silicate (Table 1).

The need for internal consistency leaves us with a two-fold conclusion: if large interstellar dust particles consist of compact silicates with optical properties similar to those assumed by Landgraf *et al.* (*5*) , then our results are in conflict with the U/G observations, and consistent with astronomical observations (*44*). On the other hand, if large interstellar dust particles have low densities, which appears to be more likely based on trajectories, capture speeds and compositions of our candidates, then our data can be consistent with the U/G observations, and possibly also with the astronomical observations, depending on the (currently unknown) wavelength-dependence of the extinction cross sections of these particles. The latter conclusion is encouraging news for any future sample return missions with the goal of capturing large numbers of relatively intact interstellar dust particles.

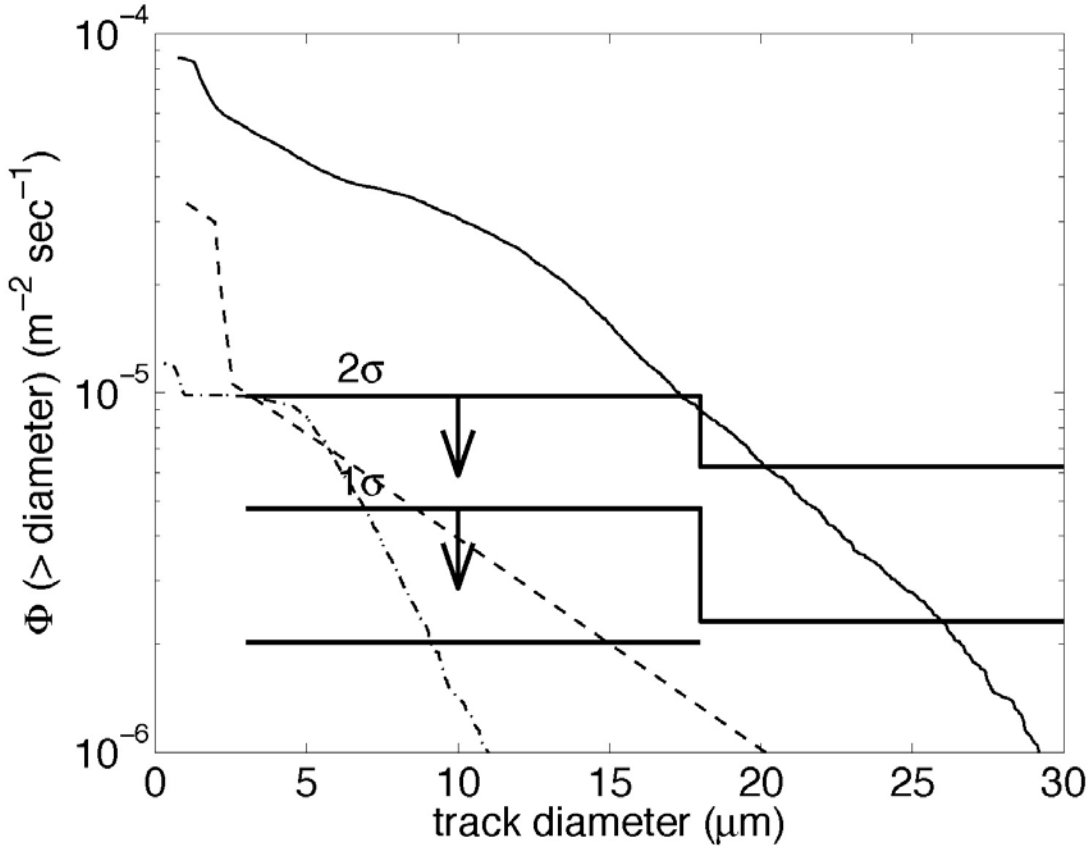

Fig. 5. Comparison of the integral track areal density as a function of diameter observed in the Stardust aerogel collectors (the lower segment is measured value, stepped curves are 1σ and 2σ upper limits) with the predictions of a model based on Ulysses and Galileo *in situ* observations, an empirical model of track diameter versus particle diameter and capture speed derived from laboratory calibrations (*13*), and a standard model of β versus particle size (*5*) (solid curve). The dashed curve is a similar prediction based on work done under the ISPE (*18*), which includes a model of the optical properties of ISD with larger values of β, and includes Lorentz forces. The dot-dashed curve shows the same calculation, but with β taken to be three times the standard model of Landgraf et al. (*5*).

Supplementary Materials

References and Notes

1. D. Brownlee *et al.*, Comet 81P/Wild 2 under a microscope, *Science* **314**, 1711-1716 (2006).

2. P. C. Frisch, J. D. Slavin, Interstellar dust close to the Sun, *Earth, Planets and Space* **65**, 175-182 (2013).
3. H. Kimura, I. Mann, E. K. Jessberger, Composition, structure, and size distribution of dust in the local interstellar cloud, *Astrophys. J.* **583**, 314-321 (2003).
4. B. T. Draine, Interstellar dust grains, *Annual Review of Astronomy and Astrophysics* **41**, 241-289 (2003).
5. M. Landgraf, W. J. Baggaley, E. Grun, H. Kruger, G. Linkert, Aspects of the mass distribution of interstellar dust grains in the solar system from in situ measurements, *J. Geophys. Res. Space Phys.* **105**, 10343-10352 (2000).
6. E. Grün *et al.*, Discovery of Jovian Dust Streams and Interstellar Grains by the Ulysses Spacecraft, *Nature* **362**, 428-430 (1993).
7. H. Krueger *et al.*, Three years of Ulysses dust data: 2005 to 2007, *Planet. Space Sci.* **58**, 951-964 (2010).
8. All particle sizes heareafter are given in diameter, rather than radius.
9. A. J. Westphal *et al.*, Stardust Interstellar Preliminary Examination I: Identification of tracks in aerogel, *Meteorit. Planet. Sci.* **in press**.
10. D. R. Frank *et al.*, Stardust Interstellar Preliminary Examination II: Curating the interstellar dust collector, picokeystones, and sources of impact tracks, *Meteorit. Planet. Sci.* **in press**.
11. H. A. Bechtel *et al.*, Stardust Interstellar Preliminary Examination III: Infrared spectroscopic analysis of interstellar dust candidates, *Meteorit. Planet. Sci.* **in press**.
12. A. L. Butterworth *et al.*, Stardust Interstellar Preliminary Examination IV: Scanning Transmission X-ray Microscopy analyses of impact features in the Stardust Interstellar Dust Collector, *Meteorit. Planet. Sci.* **in press**.
13. F. E. Brenker *et al.*, Stardust Interstellar Preliminary Examination V: XRF analyses of interstellar dust candidates at ESRF ID13, *Meteorit. Planet. Sci.* **in press**.
14. A. S. Simionovici *et al.*, Stardust Interstellar Preliminary Examination VI: Quantitative elemental analysis by synchrotron X-ray fluorescence nanoimaging of eight impact features in aerogel, *Meteorit. Planet. Sci.* **in press**.
15. G. J. Flynn *et al.*, Stardust Interstellar Preliminary Examination VII: Synchrotron X-ray fluorescence analysis of six stardust interstellar candidates measured with the advanced photon source 2-ID-D microprobe, *Meteorit. Planet. Sci.* **in press**.
16. Z. Gainsforth *et al.*, Stardust Interstellar Preliminary Examination VIII: Identification of crystalline material in two interstellar candidates, *Meteorit. Planet. Sci.* **in press**.
17. F. Postberg *et al.*, Stardust Interstellar Preliminary Examination IX: High-speed interstellar dust analog capture in Stardust flight-spare aerogel, *Meteorit. Planet. Sci.* **in press**.
18. V. J. Sterken *et al.*, Stardust Interstellar Preliminary Examination X: Impact speeds and directions of interstellar grains on the Stardust dust collector, *Meteorit. Planet. Sci.* **in press**.
19. R. M. Stroud *et al.*, Stardust Interstellar Preliminary Examination XI: Identification and elemental analysis of impact craters on Al foils from the Stardust Interstellar Dust Collector, *Meteorit. Planet. Sci.* **in press**.

20. A. J. Westphal *et al.*, Final reports of the Stardust Interstellar Preliminary Examination, *Meteorit. Planet. Sci.* **in press**.
21. Supplementary details are available on Science online.
22. A. T. Kearsley *et al.*, Dust from comet Wild 2: Interpreting particle size, shape, structure, and composition from impact features on the Stardust aluminum foils, *Meteorit. Planet. Sci.* **43**, 41-73 (2008).
23. A. J. Westphal *et al.*, Aerogel keystones: Extraction of complete hypervelocity impact events from aerogel collectors, *Meteorit. Planet. Sci.* **39**, 1375-1386 (2004).
24. P. Tsou, D. E. Brownlee, S. A. Sandford, F. Horz, M. E. Zolensky, Wild 2 and interstellar sample collection and Earth return, *Journal of Geophysical Research-Planets* **108**, (2003).
25. S. A. Sandford *et al.*, Assessment and control of organic and other contaminants associated with the Stardust sample return from comet 81P/Wild 2, *Meteoritics & Planetary Science* **45**, 406-433 (2010).
26. M. C. Price *et al.*, Comet 81P/Wild 2: The size distribution of finer (sub-10 μm) dust collected by the Stardust spacecraft, *Meteorit. Planet. Sci.* **45**, 1409-1428 (2010).
27. M. C. Price *et al.*, Stardust interstellar dust calibration: Hydrocode modeling of impacts on Al-1100 foil at velocities up to 300 km s-1 and validation with experimental data, *Meteorit. Planet. Sci.* **47**, 684-695 (2012).
28. J. P. Bradley, Chemically anomalous, preaccretionally irradiated grains in interplanetary dust From comets, *Science* **265**, 925-929 (1994).
29. L. P. Keller, S. Messenger, On the origins of GEMS grains, *Geochim. Cosmochim. Acta* **75**, 5336-5365 (2011).
30. P. C. Frisch *et al.*, Decades-long changes of the interstellar wind through our solar system, *Science* **341**, 1080-1082 (2013).
31. V. Dikarev, E. Grün, M. Landgraf, W. J. Baggaley, D. P. Galligan, in *Proceedings of the Meteoroids 2001 Conference,* B. Warmbein, Ed. (2001), vol. 495, pp. 609-615.
32. M. Landgraf, M. Müller, E. Grün, Prediction of the in-situ dust measurements of the Stardust mission to comet 81P/Wild 2, *Planet. Space Sci.* **47**, 1029-1050 (1999).
33. M. J. Burchell, M. J. Cole, M. C. Price, A. T. Kearsley, Experimental investigation of impacts by solar cell secondary ejecta on silica aerogel and aluminum foil: Implications for the Stardust Interstellar Dust Collector, *Meteorit. Planet. Sci.* **47**, 671-683 (2012).
34. N. Gehrels, Confidence limits for small number events in astrophysical data, *Astrophys. J.* **303**, 336-346 (1986).
35. H. Krüger, E. Grün, Interstellar dust inside and outside the heliosphere, *Space Sci. Rev.* **143**, 347-356 (2009).
36. M. Min, J. W. Hovenier, L. B. F. M. Waters, A. de Koter, The infrared emission spectra of compositionally inhomogeneous aggregates composed of irregularly shaped constituents, *Astronomy & Astrophysics* **489**, 135-141 (2008).
37. E. B. Jenkins, A unified representation of gas-phase element depletions in the interstellar medium, *Astrophysical Journal* **700**, 1299-1348 (2009).
38. F. Kemper, W. J. Vriend, A. G. G. M. Tielens, The absence of crystalline silicates in the diffuse interstellar medium, *Astrophys. J.* **609**, 826-837 (2004).

39. F. Kemper, W. J. Vriend, A. Tielens, Errata: The absence of crystalline silicates in the diffuse interstellar medium (**609**, p. 826, 2004), *Astrophys. J.* **633**, 534-534 (2005).
40. A. P. Jones, J. A. Nuth, Dust destruction in the ISM: a re-evaluation of dust lifetimes, *Astron. Astrophys.* **530**, 44 (2011).
41. F. J. Molster, L. Waters, The mineralogy of interstellar and circumstellar dust, *Astromineralogy* **609**, 121-170 (2003).
42. S. Messenger, L. P. Keller, D. S. Lauretta, Supernova olivine from cometary dust, *Science* **309**, 737-741 (2005).
43. C. Vollmer, P. Hoppe, F. E. Brenker, C. Holzapfel, Stellar MgSiO3 perovskite: A shock-transformed stardust silicate found in a meteorite, *Astrophysical Journal* **666**, L49-L52 (2007).
44. B. T. Draine, Perspectives on interstellar dust inside and outside of the heliosphere, *Space Sci. Rev.* **143**, 333-345 (2009).
45. E. Grün, H. A. Zook, H. Fechtig, R. H. Giese, Collisional balance of the meteoritic complex, *Icarus* **62**, 244-272 (1985).
46. D. Nesvorny, D. Vokrouhlicky, W. F. Bottke, M. Sykes, Physical properties of asteroid dust bands and their sources, *Icarus* **181**, 107-144 (2006).
47. R. L. Smith, K. M. Pontoppidan, E. D. Young, M. R. Morris, E. F. van Dishoeck, High-precision (CO)-O-17, (CO)-O-18, and (CO)-O-16 measurements in young stellar objects: analogues for CO self-shielding in the early solar system, *Astrophys. J.* **701**, 163-175 (2009).
48. E. D. Young, M. Gounelle, R. L. Smith, M. R. Morris, K. M. Pontoppidan, Astronomical oxygen isotopic evidence for supernova enrichment of the solar system birth environment by propagating star formation, *Astrophys. J.* **729**, (2011).
49. L. R. Nittler, E. Gaidos, Galactic chemical evolution and the oxygen isotopic composition of the solar system, *Meteorit. Planet. Sci.* **47**, 2031-2048 (2012).
50. J. G. A. Wouterloot, C. Henkel, J. Brand, G. R. Davis, Galactic interstellar $^{18}O/^{17}O$ ratios - a radial gradient?, *Astron. Astrophys.* **487**, 237-246 (2008).
51. A. A. Penzias, The isotopic abundances of inter-stellar oxygen, *Astrophys. J.* **249**, 518-523 (1981).
52. D. Nesvorny, P. Jenniskens, H. F. Levison, W. F. Bottke, D. Vokrouhlicky, M. Gounelle, Cometary origin of the Zodiacal cloud and carbonaceous micrometeorites. Implications for hot debris disks, *Astrophys. J.* **713**, 816-836 (2010).
53. D. Jewitt, H. Weaver, J. Agarwal, M. Mutchler, M. Drahus, A recent disruption of the main-belt asteroid P/2010A2, *Nature* **467**, 817-819 (2010)
54. H. H. Hsieh, D. Jewitt, P. Lacerda, S. C. Lowry, C. Snodgrass, The return of activity in main-belt comet 133P/Elst-Pizarro, *MNRAS* **403**, 363-377 (2010)

Acknowledgments: The ISPE consortium gratefully acknowledges the NASA Discovery Program for Stardust, the fourth NASA Discovery mission. NASA grants supported the following authors: NNX09AC36G—AJW, ALB, ZG, RL, DZ, WM and JVK; NNX09AC63G—CF, RD, AL, WJO, KS and FJS; NNH11AQ61I—RMS, HCG and NDB; NNX11AC21G—AMD, AJK, and TS; NNX11AE15G—GJF. The Advanced Light Source and the National Center for Electron Microscopy are supported by the Director, Office of Science, Office of Basic Energy Sciences, of the U.S. Department of Energy (DOE) under Contract No. DE-AC02-05CH11231. Use of the National Synchrotron Light Source, Brookhaven National Laboratory, was supported by the U.S. Department of Energy, Office of Science, Office of Basic Energy Sciences, under Contract No. DE-AC02-98CH10886. Use of the Advanced Photon Source, an Office of Science User Facility operated for the U.S. DOE Office of Science by Argonne National Laboratory, was supported by the U.S. DOE under Contract No. DE-AC02-06CH11357. MT and FP acknowledge support by Klaus Tschira foundation. AA, BH and PRH were supported by the Tawani Foundation. MJB and MCP are supported by STFC (UK). FEB, JKH, PH, JL, FP, SS, RS, MT were supported by funding of the German Science Foundation (DFG) within SPP1385: the first ten million years of the solar system - a planetary materials approach. The ESRF ID13 measurements were performed in the framework of ESRF LTP EC337, with financial support by the Funds for Scientific Research (FWO), Flanders, Belgium (contract nr. G.0395.11, G.0257.12N and Big Science programme G.0C12.13). G. Silversmit was postdoctoral fellow of the FWO during the ISPE investigations. Data described in this paper are described in the Supplementary Material and in references 9-20.